ОБЪЕДИНЕННЫЙ
ИНСТИТУТ
ЯДЕРНЫХ
ИССЛЕДОВАНИЙ

Дубна

E14-98-186

H.Huber[1], W.Assmann[1], S.A.Karamian, H.D.Mieskes[1],
H.Nolte[1], E.Gazis[2], M.Kokkoris[2], S.Kossionides[2],
R.Vlastou[2], R.Grötzschel[3], A.Mücklich[3], W.Prusseit[4]

HEAVY-ION INDUCED DAMAGE OF CRYSTALLINE Ge AND W AT 0.5 TO 8 A·MeV RANGE

Submitted to the Proceedings of SHIM-98 Symposium,
May, 1998, Berlin, Germany

[1]Sektion Physik, Ludwig-Maximilians Univ., München, Germany
[2]NRCPS «Demokritos» and NTU, Athens, Greece
[3]Forschungszentrum Rossendorf, Dresden, Germany
[4]TU, München, Germany

1998

1. Introduction

Radiation damage in metals and semiconducting crystals has been studied for many years at energies in the 100 keV region. Heavy-ion induced damage in the range of high energy is a new branch of radiation physics. While performing experiments at high energies one has to bear in mind the variety of effects observed at low energy implantation (such as sensitivity of the resulting damage to the experimental conditions) in addition to probable manifestation of new effects arising only for high energy ions. Among the latter some are already observed, i.e. a sponge-like porous structure formation in a deep layer of Ge [1] and defect annealing induced by the electronic energy-loss [2].

Astonishing modifications were also found in amorphous and polycrystalline materials /3-5/ and the thermal-spike model was supported experimentally /6,7/. The reference list cannot be complete because of the limited volume of the present paper and only a few important effects are mentioned now: First an active role of the defect clusters as sinks and sources of mobile defects /8,9/, second the influence of the implantation temperature /10,11/ and third the dose-rate dependence of the damage /12,13/.

The main objective of the present work is the comparison of the damage behaviour induced in Ge and W crystals by a variety of heavy ions in the energy range (0.3-8.0) · A MeV. The studied crystals are among the best samples for blocking and channeling, but they are unlike each to another both in their crystallographic structure and macroscopic properties.

2. Experimental

The present results have been obtained by three groups working (partially in collaboration) at Munich, Dubna and Athens. The experimental setups description and preliminary results were published elsewhere /14-16/. The "Demokritos" (Athens) experiment was performed at the electrostatic accelerator using the RBS channeling method with C and O ion beams. In Dubna the heavy-ion cyclotron was used for the elastic recoil detection (ERD) experiment, while the blocking patterns have been recorded by solid state track detectors. The ERD system at the Munich 15 MV Tandem contains a beam collimator, a computer-controlled goniometer for the target rotation (2 degrees of freedom) and translation (2 more) and a two-dimensional position sensitive ionization chamber with ΔE-E_{rest} identification of recoiling particles. The ionization chamber has the resolution of about 1% in energy, less than 0.1° in scattering angles and a charge discrimination less than 1 for nuclei with Z up to 30. The kinematic corrections in energy by the position signals are introduced automatically in the software. The data are accumulated event by event and processed on- or offline to give a two-dimensional blocking pattern.

Polished and etched Ge and W plates of about 0.5 mm thickness were glued upon the goniometer platform and used as targets. The irradiations were performed at room temperature at the vacuum of 10^{-7} Torr. The maximum fluence was reached typically after 10 hr irradiation. In all experiments no carbon build-up could be detected. The macroscopic temperature of the target active volume was not changed by the beam since its thermal power was on the level of only 0.1 W. The beam intensity was distributed more or less uniformly over a 1x1 mm^2 spot.

The minimum yield χ_m and angular half-width $\psi_{1/2}$ of the blocking dip were measured as a function of fluence and beam density. At the beginning of irradiation the best contrast blocking pattern has been observed, thus the damaging effect could be seen clearly. The results of all irradiations (Table 1) are finally used for the systematization of the damaging efficiency of heavy ions.

3. Results

The blocking minimum parameters are influenced by finite thickness of the target layer and they are dependent on Z and E of the detected particle etc. Thus, for the correct comparison of different irradiations the defect concentration n_D has to be deduced. A special program was developed in order to calculate the damage dependent dechanneling fraction in the multiple-scattering model and to deduce the n_D value from the fit to the measured χ_m and $\psi_{1/2}$ parameters. Schematically this program can be compared with others used in literature, for instance /17/, but the multiple-scattering role is taken into account in a different manner. The χ_m measured for a damaged crystal contains a few components corresponding to all imperfections in a virgin crystal + the yield of scattering on statically displaced atoms + the yield change due to dechanneling (deblocking) during a particle's path through the damaged crystal layer. As known from [18] the measured $(1-\chi_m)$ value is expressed as a product of the corresponding values for all fractional components. Thus, one can distinguish three basic components noted above and write the following expression:

$$1 - \chi_m(\phi) = [1 - \chi_m(0)]\,[1 - n_D(\phi)]\,[1 - F(n_D \cdot s)], \qquad (1)$$

where $\chi_m(0)$ and $\chi_m(\phi)$ are the yields measured for the virgin and after exposure to a fluence ϕ crystals, respectively. n_D is the defect concentration and F is the dechanneled fraction dependent on n_D and the layer thickness, s. From eq. (1) one finds immediately:

$$n_D = \frac{\chi_m(\phi) - \chi_m(0) - F + F \cdot \chi_m(0)}{1 - \chi_m(0) - F + F \cdot \chi_m(0)} \qquad (2)$$

The multiple-scattering (MS) model is used for the evaluation of the dechanneling component F. Assume that the MS angle after a pathlength s in the damaged crystal can be substituted for that calculated with the pathlength $n_D \cdot s$ in an amorphous material.

This approximation is valid both for the case of randomly distributed point defects and for the sample containing $(1-n_D)$ portion of the nondamaged crystalline material and n_D portion of the amorphous one. The Bohr formula for the MS angle is used with a normalizing constant C, which is a free parameter of the model:

$$\psi_{1/2}^{MS} = \Omega\sqrt{\ln 2} = C\sqrt{2\pi \ln 2}\left(\frac{Z_1 Z_2 e^2}{E}\right)\sqrt{N \cdot n_D \cdot s \ln(1.29\varepsilon)} \qquad (3)$$

where Z_1, E and ε are the atomic number, the laboratory energy and reduced energy of the particle, respectively. Z_2 and N are the atomic number and atomic density of the matrix material. The blocking minimum shape can be approximated by a Gaussian, and cylindrically symmetric Gaussian distribution of the MS angle has to be combined with the cylindrically symmetric (in the axial case) blocking-effect distribution. A new Gaussian distribution of emitted particles arises which is characterized by the angular width:

$$\left(\psi_{1/2}^{f}\right)^2 = \left(\psi_{1/2}^{i}\right)^2 + \left(\psi_{1/2}^{MS}\right)^2$$

Applying the requirement of blocking dip volume conservation [19], the minimum yield increase due to MS can be calculated also, and the $F(n_D s)$ function is deduced as follows:

$$F = \left(\psi_{1/2}^{MS}\right)^2 \cdot \left[\left(\psi_{1/2}^{i}\right)^2 + \left(\psi_{1/2}^{MS}\right)^2\right]^{-1}. \qquad (4)$$

The values of $\chi_m(\phi)$ and $\psi_{1/2}(\phi)$ are taken at a number of fluence points. From $\chi_m(\phi)$ one can deduce the corresponding $n_D(\phi)$ value using eqs. (2-4). Iterations have to be applied since the F function in eq. (2) is dependent on n_D. The finally determined n_D and MS angle values allow one to evaluate the $\psi_{1/2}^{f}$ value and compare it with the experimentally measured $\psi_{1/2}(\phi)$values. The latter procedure ensures control that the results are reproduced successfully in the MS model. In Fig.1 the results of quantitative simulations of the blocking minimum parameters in the MS model are shown together with the experimental points. The predicted $\psi_{1/2}(\phi)$ behaviour is compared with the measured values as well. The agreement is good for the examples illustrated in Fig.1, and also (within the limits of experimental errors) for all other irradiations. The only free parameter of the model in eq. (3) was chosen to be C=0.45 in order to get the best overall fit to the total set of experimental points for both crystals. In Figs.2 and 3 additional results from the W and Ge crystals

damage are presented. The n_D (ϕ) curves for W (Fig.2) show more or less regular scaling. However, the results for Ge demonstrate a surprisingly low level saturation of damage for very heavy ion irradiations (I, Xe) and a dose-rate dependence of the damage functions (Fig.3). These peculiarities has to be explained, and an attempt to give the realistic interpretation is undertaken below.

4. Discussion

The simplest model predicting the saturation of the defect concentration at a level below 1 as well as the dose-rate dependence of the n_D (ϕ) function is known from ref. /20/:

$$dn_D/dt = R\,(1 - n_D) - \alpha\, n_D; \qquad (5)$$

$$n_D = \frac{R}{R+\alpha}\left[1 - e^{-(R+\alpha)t}\right], \qquad (6)$$

where R is the rate of displacement due to atomic collisions and $\alpha(T)$ is the coefficient of the temperature induced recombination of free defects. It can be applied to the description of the n_D (ϕ) functions for tungsten. However, at the case of Ge crystal the situation is more complicated. For any ion species eq. (6) predicts a constant level of saturation as far as R is kept constant. As clear from present measurements this doesn't take place in reality, see for instance, Figs.1a and 3.

One possible modification is the introduction of the term ($-\beta\, n_D$) into eq. (5) which means the additional annealing due to the electronic-energy losses S_e of heavy ions. Thus, n_D is expressed as follows:

$$n_D = \frac{R}{R+\beta+\alpha}\left[1 - e^{-(R+\beta+\alpha)t}\right]. \qquad (7)$$

The coefficient β (S_e) being dependent on the ion species can provide the description of the set of n_D (ϕ) functions for all ions. The eqs. (6) and (7) can be successfully applied to description of the $n_D(\phi)$ functions for W crystal and for any other cases where collisional mechanism is valid. There are still some doubts in the justice of such simple phenomenolagical models for any crystal species and irradiation conditions. The microscopical behaviour of the point defects in the crystal medium at finite temperature under the beam has to be ascribed in theory. Some attempts of the microscopical approach are known starting from ref. /8/. Unfortunately, the decisive progress in such theories was not achieved until now.

In a semiphenomenological approach one can try to take into account the processes of the mobile defects production and interaction, their stabilization in form of isolated defects and defect

clusters as well as the elution of mobile defects from clusters by the beam. The corresponding differential equation looks like:

$$r = R\,(1 - n_D)[1 + \alpha\,(n_D)^{5/6}]; \qquad (8)$$

$$\frac{dn_D}{dt} = \lambda_1 r^{3/2} + \lambda_2 r (n_D)^{5/6} - \alpha R (1 - n_D)(n_D)^{5/6}, \qquad (9)$$

where r is the rate of newly produced mobile defects and the terms proportional to $(n_D)^{5/6}$ are responsible for the defect capture and elution in interaction with clusters. The failure of this approach is lack of data for the realistic choice of numerical values of parameters in eqs. (8, 9). For the qualitative analysis eq. (8) was substituted into (9) and the differential equation was solved by the method of computer integration. The resulting function n_D (t) is applicable for description of the experimentally measured $n_D(\phi)$ functions. The comparison of the experimental points with the fit, using eq. (9) is shown for example in Fig. 3. This means that the experimental results donot contradict to the model taking into account the recombination, clusterization and beam-induced mobility of defects. However, it is obviously impossible to specify the scenario of the elementary defect fate basing only on measured n_D (ϕ) functions.

Eqs. (5, 8) and all similar models predict the start point derivative dn_D/dt=R at t=0. This means that the slope of the $n_D(\phi)$ function at (ϕ) near 0 cannot deviate from the displacement rate predicted by theory, because this approach considers the random migration and interaction of homogeniously distributed defects as an initial stage and doesnot involve at all the processes within the microvolume of wake excitations produced by single ion. In the latter volume the microtemperature can be significantly different from the sample temperature as well as the defect concentration never streams to zero, just to some finite limit (low enough for swift ions) defined by the displacement cross-section.

By these reasons the account of the energy-loss-induced recombination in eq. (7) is a nonsatisfactory approximation, and the set of data on Ge damage has to be analyzed using another assumption. The damaging efficiency at low fluences may throw some light on processes within the volume perturbed by single ion. In previous experiments /2, 4, 7/ some indications of the defect selfannealing were found, and now more results are available for Ge (Table). The slope $dn_D/d\phi$ at low fluences appears to be the correct parameter of the ion damaging power. The number of displacements generated in the atomic collision cascade has been simulated by the Monte-Carlo code TRIM. Finally, the ratio of the experimentally determined $dn_D/d\phi$ values and the TRIM-predicted displacements is plotted versus electronic stopping parameter (calculated using the same code), as shown in Fig.4.

An order magnitude decrease in the relative damaging power (damaging efficiency) can be explained only by the defect annealing due to high electronic energy loss. Scattering of the points in Fig.4 is due to both experimental errors and dose rate effect. Despite the points scattering the general trend of the damaging power decrease with S_e parameter is evident and three group's results are in a reasonable agreement.

The large amount of energy released during ion penetration (up to 30 MeV/μm in this case) is enough to produce heating of the material near the ion trajectory.This was shown in theoretical estimations and was confirmed experimentally. The individual ion temperature spike has an estimated short lifetime $\tau<0.1$ ns. To be effective within such a short time the annealing temperature has to be at least a few hundred degrees C. Thermal spike induced crystallization [5] produces a detectable track contrast in the amorphous Si and Ge. And the recrystallization process in the single crystal surroundings leads naturally to the restore of the lattice. The rapid selfannealing process defines the slope $dn_D/d\phi$ at low fluences and the defect migration, recombination and clusterization are significant on the late stages.

For tungsten crystal the measured damaging power values are proportional to the TRIM predicted displacements. Thus, within the experimental errors the influence of electronic stopping onto W damage is not revealed unlike to the Ge damage. The saturation of the $n_D(\phi)$ functions can be explained satisfactory by the recombination of point defects in W case.

Conclusions

Swift-ion induced damage in Ge and W crystals is systematically studied. The observed disorder saturation (at high fluences) and dose-rate dependence can be explained by the defect mobility and recombination processes with possible role of the clusterization and beam-induced elution of defects from clusters. The damaging efficiency decreases significantly for very heavy ions in Ge, thus, electronic energy-loss-induced selfrecrystallization is evident in Ge and not in W. Wake recrystallization accomplishes the latent track formation and bound phenomena, all connected with processes in the microvolume excited by the single-ion passage. The resulting lattice restore, however, looks like the inversion in comparison with the disordering in the latent track.

Acknowledgements

The stimulating discussions with Professors J.Forster, S.Klaumünzer, M.Toulemonde and Dr. D.Avasthi are gratefully acknowledged. One of authors (S.A.K.) is grateful to the DLR IB/OVB office (Germany) for the support of the JINR-LMU collaboration.

Table. Parameters of irradiations

Crystal	Projectile	Energy, MeV	Incidence angle, deg	Detected particle	Scattering angle, deg	Maximum dose, (10^{14}cm^{-2})	Dose rate, (10^{11}cm^{-2} c^{-1})	Institute
Ge(100)	^{12}C	12	0	C	160	2.0	8.3	"Demokritos"
Ge(100)	^{16}O	18	0	O	160	1.2	5.0	"Demokritos"
Ge(111)	^{20}Ne	12	50	Ne	130	0.56	5.3	JINR, Dubna
Ge(111)	^{20}Ne	104	41.5	Ge	68	1.5	4.0	JINR, Dubna
Ge(100)	^{32}S	90	75.3	S	50.2	1.3	1.6	LMU, Garching
Ge(111)	^{40}Ar	25	38.5	Ar	71	0.29	2.8	JINR, Dubna
Ge(100)	^{58}Ni	165	75.3	Ge	50.2	0.5	1.0	LMU, Garching
Ge(111)	^{63}Cu	35	56.5	Ge+Cu	53	0.15	1.0	JINR, Dubna
Ge(111)	^{84}Kr	73	50.5	Ge(Kr)	59	0.32	1.2	JINR, Dubna
Ge(100)	^{127}I	185	75.3	Ge	50.2	0.15	0.3 and 1.3	LMU, Garching
Ge(100)	^{127}I	210	75.3	Ge	50.2	0.12	0.4 and 1.2	LMU, Garching
Ge(111)	^{136}Xe	56	56.5	Ge	53	0.07	0.2	JINR, Dubna
Ge(111)	^{136}Xe	116	50.5	Ge	59	0.09	0.3	JINR, Dubna
Ge(111)	^{129}Xe	124	45.5	Ge	64	0.30	0.9	JINR, Dubna
Ge(100)	^{197}Au	100	75.3	Ge	50.2	0.05	0.43	LMU, Garching
Ge(100)	^{197}Au	252	75.3	Ge	50.2	0.10	0.29	LMU, Garching
Ge(100)	^{197}Au	266	75.3	Ge	50.2	0.05	0.28	LMU, Garching
W(110)	^{16}O	137	51	f. f.	164	4.6	12	JINR, Dubna
W(110)	^{22}Ne	175	56	f. f.	159	1.8	4.5	JINR, Dubna
W(100)	^{32}S	175	75	S	50.2	1.7	4.8	LMU, Garching
W(110)	^{40}Ar	25	56	Ar	159	0.6	2.5	JINR, Dubna
W(110)	^{129}Xe	124	54	W(Xe)	67	0.12	0.8	JINR, Dubna

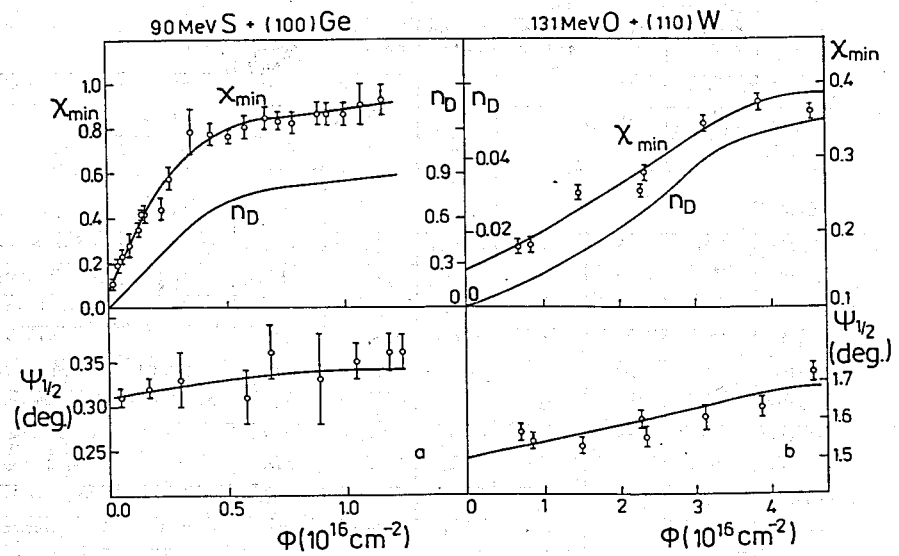

Fig.1. Fluence dependence of the blocking parameters and deduced defect concentration values for the S ion induced damage in Ge and O ion induced damage in W. The results of the fit within the MS model (eqs. (2-4)) are shown by curves.

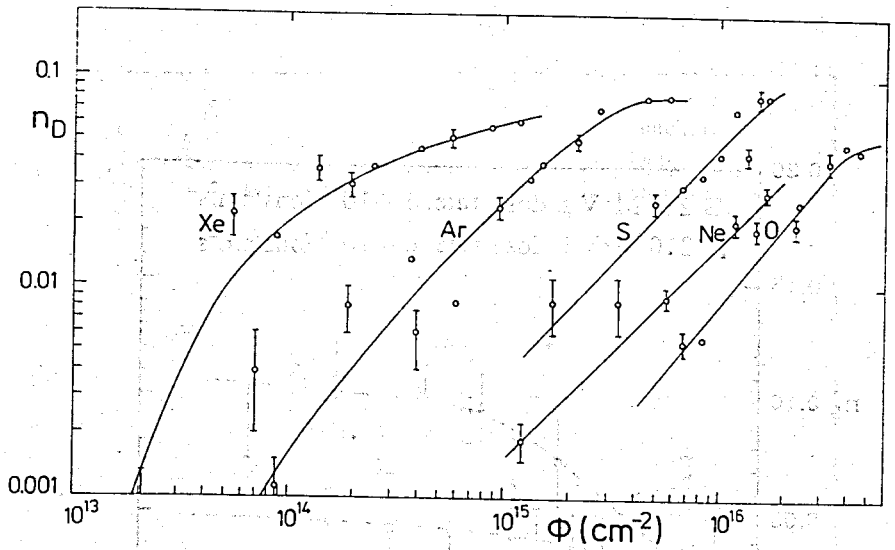

Fig.2. Defect concentration functions measured for heavy-ion irradiations of the W crystal. Parameters of irradiations are given in the Table .

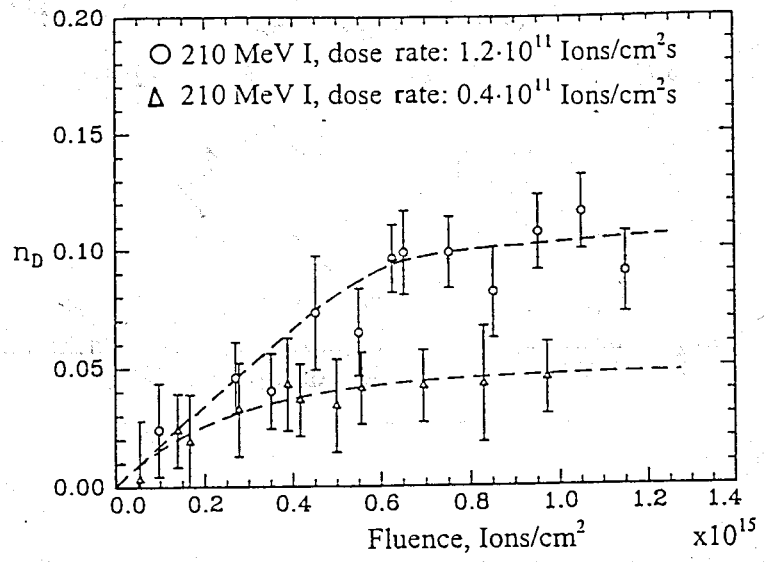

Fig.3. Damage versus dose dependencies taken at the 210 MeV I ion irradiations of the Ge crystal at two values of the beam density.

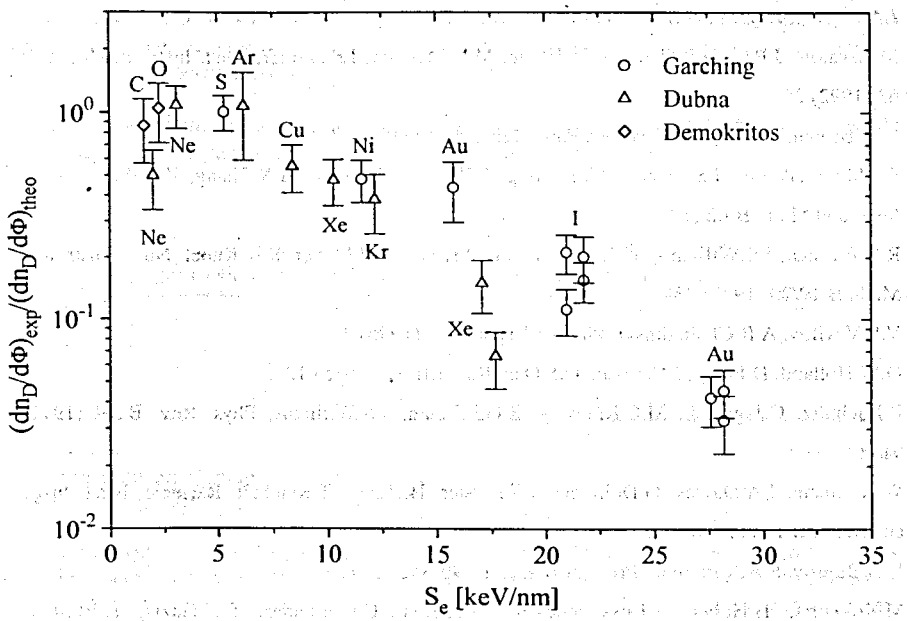

Fig.4. Systematics of the heavy-ion damaging efficiency as a function of the electronic stopping parameter for the Ge crystal normalized to unity for light ions.

References

1. H.Huber, W.Assmann, S.A.Karamian, A.Müklich, W.Prusseit, E.Gazis, R.Grötzschel, M.Kokkoris, E.Kossionides, H.D.Mieskes, R.Vlastou, Nucl. Instr. and Meth. B 122 (1997) 542.
2. S.A.Karamian, Yu.Ts.Oganessian, V.N.Bugrov, Nucl. Instr. and Meth. B 43 (1989) 153.
3. S.Klaumünzer, G.Schumacher, Phys. Rev. Lett. 51 (1983) 1987.
4. A.Dunlop, D.Lesueur, J.Dural, Nucl. Instr. and Meth. B 42 (1989) 182.
5. S.Furuno, H.Otsu, K.Hojou, K.Izui, Nucl. Instr. and Meth. B 107 (1996) 223.
6. M.Toulemonde, J.Dural, G.Nouet, P.Mary, J.F.Hamet, M.F.Beaufort, J.C.Desoyer, C.Blanchard, J.Auleyther, Phys. Stat. Sol. A 114 (1989) 467.
7. M.Levalois, J.P.Girard, G.Allais, A.Hairie, M.N.Metzner, E.Paumier, Nucl. Instr. and Meth. B 63 (1992) 25.
8. L.M.Brown, A.Kelly, R.M.Mayer, Phil. Magazine 19 (1969) 721.
9. R.J.Shreutelkamp, J.S.Custer, J.R.Liefting, F.W.Saris, W.X.Lu, B.X.Zhang, Z.L.Wang, Nucl. Instr. and Meth. B 62 (1992) 372.
10. R.G.Elliman, J.S.Williams, W.L.Brown, A.Leiberich, D.M.Maher, R.V.Knoel, Nucl. Instr. and Meth. B 19/20 (1987) 435.
11. V.S.Vavilov, A.R.Cheliadinski, Physics-Uspekhi 38 (1995) 333.
12. O.W.Holland, D.Fathy, J.Narayan, O.S.Oen, Rad. Eff. 90 (1985) 127.
13. P.J.Schultz, C.Jagadish, M.C.Ridgway, R.G.Elliman, J.S.Williams, Phys. Rev. B 44 (1991) 9118.
14. W.Assmann, J.A.Davies, G.Dollinger, J.S.Forster, H.Huber, T.Reichelt, R.Sigele, Nucl. Instr. and Meth. B 118 (1996) 242.
15. V.N.Bugrov, S.A.Karamian, Preprint JINR P14-90-352 (1990).
16. M.Kokkoris, H.Huber, S.Kossionides, T.Paradellis, Ch.Zarkadas, E.N.Gazis, R.Vlastou, X.Aslanoglou, W.Assmann, S.A.Karamian, Proc. 14-th Intern. Conf. on Applications of Accclerators, Denton, ed. J.L.Duggan, AIP Press, N.Y. (1997) 455.
17. J.F.Ziegler, J.Appl. Phys. 43 (1972) 2973.
18. S.A.Karamian, Sov. J. Particles and Nuclei 17 (1986) 753.
19. F.Malaguti, S.Ostuni, E.Verondini, E.Fuschini, G.Vanini, I.Iori, A.Bracco, A.Moroni, E.Fioretto, R.A.Ricci, P.Boccaccio, L.Vannucci, Europhys. Lett. 12 (1990) 313.
20. F.L.Vook, H.J.Stein, Rad. Eff. 2 (1969) 23.
21. S.A.Karamian, Nucl. Instr. and Meth. B 51 (1990) 354.

Received by Publishing Department
on June 24, 1998.